A Power Allocation Strategy for Multiple Poisson Spectrum-Sharing Networks

Ran Cai, *Student Member, IEEE*, Jian-Kang Zhang, *Senior Member, IEEE*, Timothy N. Davidson, *Member, IEEE*, Wei Zhang, *Fellow, IEEE*, Kon Max Wong, *Life Fellow, IEEE*, and P. C. Ching, *Fellow, IEEE*

Abstract—This paper develops a power allocation strategy for multiple networks of Poisson-distributed single-antenna nodes that share the available spectrum in a spectrum underlay scenario. This strategy aims to maximize the overall throughput obtained by sharing the spectrum while limiting the degradation of the successful transmission probability of each network. In its original form, this joint power allocation problem is difficult to solve. However, we demonstrate that the problem can be transformed into a convex optimization formulation, which can be efficiently solved. Furthermore, we obtain a quasi-closed-form solution that has a water-filling interpretation by analyzing the optimality conditions. Numerical results indicate that, when a spectrum-sharing scheme employs the proposed optimal strategy of power allocation, the throughput substantially improves over that obtained by exclusively allocating the spectrum to the primary network. Moreover, when the number of spectrum-sharing networks increases, the enhancement is significant, being up to the limit imposed by the maximum allowable degradation in the performance of each network.

Index Terms—Spectrum sharing, power allocation, convex optimization, stochastic geometry, spatial networks.

I. INTRODUCTION

SPECTRAL utilization can be enhanced by enabling the concurrent operation of two or more networks [1], [2]. This spectrum sharing mode is often referred to as spectrum underlay. This paper focuses on spectral underlay systems in which the spectrum is shared between a licensed primary network (PN) and multiple unlicensed secondary networks (SNs). The access of the PN to the spectrum is to be guaranteed, whilst secondary users can access the band as long as their interference

with each network does not exceed a tolerable limit. This limit may either take the form of a hard interference constraint that must always be maintained, such as the limit of interference temperature [3], or of a soft interference constraint that is based on probabilistic measures of interference [4], [5]. This paper aims to allocate transmission power to each network in a way that maximizes the sum of the throughput of each network, subject to probabilistic constraints on the impact of interference on each network. (The throughput of a network is defined as the product of the rate per unit area and the corresponding probability that the idealized transmission is successful at that rate.)

A. Motivations and Related Works

1) Power Allocation Strategies: In spectrum sharing networks, power allocation is critical to interference management. Recent works (e.g., [6]–[10]) have demonstrated that judicious power allocation schemes can improve the overall spectral utilization substantially while maintaining specified levels of quality-of-service (QoS) in each network. However, most of the existing schemes have been developed for finite and deterministic networks in which either channel state information (CSI) or user location is assumed.

In practice, these schemes can be quite difficult to implement because the available CSI must be sufficiently accurate to protect the QoS requirements of the PN, and to ensure that those of the SNs are degraded only marginally. In some scenarios, this CSI can be difficult to obtain, such as when the PN and the SNs do not cooperate explicitly. Furthermore, the fraction of available resources that must be allocated for channel estimation and the communication of channel information can become unreasonably large. These effects can significantly reduce capacity in spectrum sharing networks (e.g., [9], [11], [12]). Even if robustness to inaccuracy in available information is explicitly incorporated into the designs (e.g., [10], [13]–[15]), substantial resources are still required to exchange the necessary information.

An alternative is to utilize instantaneous location information of the nodes in the spectrum sharing networks because some components of the CSI are dependent on the relative spatial relationships of transmitter-receiver pairs. The location information of primary users can enhance the detection of access opportunity and spectrum sharing capacity [16], [17]. In practice, however, reliable user location can be rather difficult to obtain especially for large-scale networks, due to the irregular deployment of infrastructure (cellular) networks or the user mobility of infrastructureless (*ad hoc*) networks.

2) Stochastic Geometry of Wireless Networks: In this work we adopt a different approach and devise a power allocation strategy that does not require instantaneous CSI or location information. Instead, our strategy is based on stochastic models for the geometry of the networks. From the perspective of an individual network, the positions of the nodes in the other coexisting networks can be considered spatially random; e.g., [18]–[21]. In a number of practical scenarios, the positions of those nodes can be modeled, with reasonable accuracy, by independent two-dimensional homogeneous Poisson point processes (HPPPs); e.g., [18]–[21], and we will adopt such models in our analyses. As we will show, the tractability of such models enables the development of efficient power allocation algorithms that do not require coordination between the networks. In contrast, cluster process that models coordinate nodes and hard-core process that models nodes with guard zones necessitate additional information fusion between these two kinds of nodes [18], [19].

We will consider networks in which each transmitter communicates to its corresponding receiver in a point-to-point manner, and treats all other transmissions as interference. The performance of spectrum sharing will be measured based on network-wide successful transmission probabilities that are computed for a reference transmitter-receiver pair over the random locations of the nodes in the networks and random small-scale fading.

A similar stochastic geometry model has been adopted in previous analyses of the properties of spectrum sharing networks (e.g., [22]–[27]). However, few of these works have sought insight from stochastic geometry in the development of power allocation schemes. In [28], the impact of the transmission power of secondary users on opportunity detection was quantified based on a Poisson model of the PN. In [29], the transmission power for the secondary users in a pair of random geometric networks was optimized based on energy harvesting. However, these studies focus on spectrum sharing between two networks rather than multiple networks.

3) Multiple Spectrum Sharing Networks: In this paper, we address the problem of power allocation among multiple spectrum sharing networks rather than just two. This objective is important because in many application scenarios more than two distinct networks coexist, such as concurrent transmission in the industrial, scientific, and medical (ISM) band of 2.4 GHz, including Wi-Fi, Bluetooth [30], in sensor networks and in multi-tier heterogeneous systems that involve macro-cells and micro-cells [31]–[33]. These networks are distinguished by their system parameters (e.g., network density and transmission rate) and are naturally modeled separately as different homogeneous networks instead of being considered as one large heterogeneous network. Moreover, the efficiency of spatial spectrum utilization is conditioned on the number of SNs [34]. In this paper, therefore, we seek to improve the throughput of spectrum sharing with the increase in the number of coexisting networks by allocating transmission power appropriately, up to a limit imposed by performance requirements. The two networks case is, naturally, a special case of our framework, but existing strategies for two spectrum sharing networks become ineffective for multiple networks, because the transmission power in each

network affects the overall throughput in a complicated manner. There have been only few works on forms of spectrum sharing for multiple networks. For example, [24] studied network densities of multiple spectrum sharing networks with random network structures, and [35] examined spectrum sharing among multiple parties through spectrum auction. However, the power allocation problem in multiple spectrum sharing networks has not been given much attention in previous literature.

B. Contributions

In formulating the power allocation problem for multiple spectrum sharing networks using only stochastic models for the network geometries, we analyze the increase in throughput that can be achieved and the need to alleviate the aggregate interference imposed on each network. We formulate the power allocation problem as the maximization of a sum of the throughput of each network whilst guaranteeing that the decrease in the probability of successful transmission in each network incurred by spectrum sharing is bounded by a pre-specified level. While that problem initially appears to be difficult to solve, we show that it can be transformed into a convex optimization problem that can be solved efficiently.

The main contributions of this paper can be summarized as follows.

- We propose a power allocation strategy for multiple networks rather than two networks. This strategy considers both the overall throughput of the networks and the individual performance of each network.
- We design this power allocation strategy based on the stochastic geometry model of Poisson networks. For the broad class of networks in which the node locations can be modeled using independent Poisson point processes (e.g., [18]–[20]), we derive quasi-closed-form solutions to a power allocation problem that seeks to maximize the overall throughput subject to constraints on the performance of each network. By exploiting the Poisson model, the proposed scheme effectively manages interference and increases throughput in the absence of instantaneous knowledge of channel realizations or of the instantaneous locations of nodes, thereby freeing up communication resources that could otherwise be allocated to the communication of such information.
- We show how the problem can be transformed into a convex optimization problem, even though the original formulation of the power allocation problem appears to be difficult to solve. Furthermore, we exploit the structure of this convex formulation to develop an efficient algorithm based on quasi-closed-form expressions that admit a water-filling interpretation.
- We derive the relation between the properties of each network, such as network densities and target transmission rates, and the feasible region of transmission power to facilitate the coexistence of multiple networks. Furthermore, we can determine the maximum number of spectrum sharing networks based on the feasibility condition of the spectrum sharing problem. These analytical and numerical results can significantly guide network design.
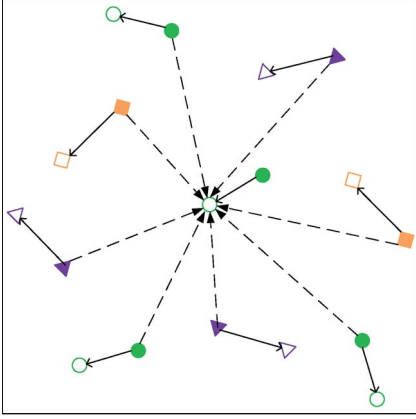
Fig. 1. Example of spectrum sharing between one primary network (circles) and two secondary networks (triangles and squares). Each network is distinguished by its system parameters; e.g. network density and transmission rate. The solid nodes denote transmitters that are distributed as independent HPPPs; the hollow nodes correspond to receivers. Solid arrows represent transmission links and dashed arrows indicate the aggregate interference towards one primary receiver.

II. SPECTRUM SHARING MODEL

We consider the scenario of underlay spectrum sharing in which one primary network (PN), referred to as network 0, and multiple secondary networks (SNs), referred to as networks $m, m = 1, 2, \ldots, M$, coexist in the same geographic region and share the same spectrum. Fig. 1 provides an example of this type of spectrum sharing among three networks. The proposed power allocation strategy is designed such that it can be implemented given low signaling overhead. It is based on a stochastic geometry model for the spatial distribution of the nodes in the networks rather than on instantaneous information on channel or node localization, and hence side information need only be exchanged when the model parameters change significantly rather than when the channel realizations change significantly.

A. Network Model

The primary network (PN) consists of multiple primary transmitters (PTs) and primary receivers (PRs), with each transmission pair communicating in a point-to-point manner and treating other transmissions as interference. The transmitters in each network are modeled as being distributed according to a two-dimensional homogeneous Poisson point process (HPPP). This stochastic geometry model [18]–[20] has been applied to large-scale *ad hoc* networks (e.g., [23]) as well as cellular networks (e.g., [21]).

In particular, we let $\Phi_0 = \{X_0^{(j)}; j = 0, 1, 2, \ldots\}$ denote the set of coordinates of PTs, where $X_0^{(j)} \in \mathbb{R}^2$ is the coordinate of the jth PT, and let λ_0 denote the spatial density of PTs (i.e., the expected number of PTs in a unit area). Due to the spatial stationarity of an HPPP,[1] the performance of the PN can be evaluated through a reference transmitter-receiver pair. For simplicity, the reference PR is selected to be located at the origin $O_0^{(0)}$. The analysis is conditioned on the fixed distance between the associated transmitter and the reference receiver, which is expressed as $R_0 = \|X_0^{(0)}\|_2$. This conditioning is common in

the literature (e.g., [22]–[25], [29]), and if a distribution for R_0 is known or postulated, the average performance over that distribution can be computed; e.g., [37].

The secondary networks (SNs) are modeled analogously. The distribution of the secondary transmitters in SN m is described by an independent HPPP of density λ_m and the set of coordinates is denoted by $\Phi_m = \{X_m^{(j)}; j = 0, 1, 2, \ldots\}$, for $m \in \{1, 2, 3, \ldots, M\}$. The SNs are distributed over the same geographical region as the PN. For SN m, the reference transmitter-receiver location pair is denoted by $(X_m^{(0)}, O_m^{(0)})$, and the associated reference transmission distance is denoted by R_m.

B. Transmission Model

In each network, each node is equipped with a single antenna and performs omnidirectional single-hop transmission. When both the large-scale path-loss and the small-scale fading are taken into account, the power $P_{a,b}$ received at receiver b from transmitter a can be modeled as

$$P_{a,b} = P_a \cdot H_{a,b} \cdot D_{a,b}^{-\alpha}, \tag{1}$$

where P_a is the transmission power at node a. We consider networks in which each transmitter in network m employs the fixed transmission power, P_m. The same assumption has been considered in [22]–[25], [29]. A feature of this class of networks is that each node in a given network has the same statistics for battery life, and this simplifies the management of network lifetime. The term $H_{a,b}$ is the small-scale fading factor from node a to node b. In the case of Rayleigh fading, $H_{a,b}$ is exponentially distributed with unit mean. All of the components of Rayleigh fading are modeled as being independent and identically distributed (i.i.d.). The term α is the path-loss exponent, $2 < \alpha < 6$, which is modeled as being constant over the region of interest. The term $D_{a,b}$ is the distance between nodes a and b. Using our notation $R_m = D_{X_m^{(0)}, O_m^{(0)}}$ for the distance between the reference transmitter and receiver pair in network m, the power of desired signal received at the reference receiver $O_m^{(0)}$ in network m is $P_{X_m^{(0)}, O_m^{(0)}} = P_m \cdot H_{X_m^{(0)}, O_m^{(0)}} \cdot R_m^{-\alpha}$. Each transmitter also generates interference to the receivers of all other networks, and in particular to the reference receivers. The interference $I_{n,m}$ from the transmitters of network $n \neq m$ to $O_m^{(0)}$ is $I_{n,m} = P_n \sum_{X_n^{(j)} \in \Phi_n} H_{X_n^{(j)}, O_m^{(0)}} \cdot D_{X_n^{(j)}, O_m^{(0)}}^{-\alpha}$. Since the interference at the reference receiver of network m is generated by the other transmitters in its own network (i.e., internal interference) and by other networks (i.e., external interference), the aggregate interference to $O_m^{(0)}$ is $I_m = \sum_{n=0}^{M} I_{n,m}$, where the expression for $I_{m,m}$ takes a similar form to that for $I_{n,m}$ above, but with the summation being over $X_m^{(j)} \in \Phi_m$ with $j > 0$.

We consider a spectrum sharing system that is interference limited, in the sense that the impact of thermal noise is negligible compared to that of interference. (While this is a commonly considered scenario, e.g., [23]–[25], the effect of noise on the performance of spectrum sharing can be determined by incorporating an extra term into (4); e.g., [37]. We will discuss

---

[1] All PRs in an HPPP network have the same statistics for signal reception [36].

this effect further in Section V.) In the interference-limited setting, the performance of each network depends on signal-to-interference ratio (SIR); i.e., $\text{SIR}_m = \frac{P_{X_m^{(0)}, O_m^{(0)}}}{I_m}$. One of the network performance criteria that we consider is a probabilistic QoS requirement. In particular, we require that a specified minimum SIR should be achieved at the reference receiver with a given probability. If we let β_m denote the SIR target for network m, the probability that the specified SIR is achieved can be written as

$$p_m = \mathbb{P}\left[\text{SIR}_m > \beta_m\right]. \tag{2}$$

This metric is adopted because the transmitting nodes in our study do not have access to channel realization; hence, they transmit at a fixed rate. If β_m denotes the SIR at which a given code can be correctly decoded with sufficiently high probability, then the probability of an outage is $1 - p_m$. For that reason, we refer to p_m as the successful transmission probability. By defining

$$b_m = \frac{2\pi^2 \beta_m^{2/\alpha} R_m^2}{\alpha} \csc\left(\frac{2\pi}{\alpha}\right) > 0, \tag{3}$$

where $\csc(\cdot)$ represents the cosecant function, and by employing the proposed statistical models for the transmitter locations and the small-scale fading, the successful transmission probability of network m, for $m = 0, 1, \ldots, M$, under the given spectrum sharing mode is

$$p_m = \exp\left[-b_m \sum_{n=0}^{M} \lambda_n \left(\frac{P_n}{P_m}\right)^{2/\alpha}\right]. \tag{4}$$

This expression can be viewed as the extension of a result in [38] for a single network to the case of multiple spectrum sharing networks. A simple proof is as follows. Starting from (2) we have that

$$p_m = \mathbb{P}\left[H_{X_m^{(0)}, O_m^{(0)}} > \frac{\beta_m R_m^\alpha I_m}{P_m}\right]$$

$$= \prod_{n=0,1,\ldots,M} \mathbb{E}_{I_{n,m}}\left[\exp\left(-\frac{\beta_m R_m^\alpha}{P_m} I_{n,m}\right)\right] \tag{5}$$

$$= \prod_{n=m=0,1,\ldots,M} \exp\left(\lambda_n \int_{\mathbb{R}^2} \frac{1}{1 + \frac{1}{\frac{\beta_m R_m^\alpha}{P_m} P_n |X_n^{(j)}|^{-\alpha}}} dX_n^{(j)}\right) \tag{6}$$

where the equality in (5) arises from the Rayleigh fading model and the equality in (6) arises from the probability-generating function of an HPPP. The expression in (4) is obtained by performing the integration in (6).

We can see from (4) that p_m is an increasing function of the power of the desired signal P_m, and a decreasing function of the transmission power of the other networks $P_n (n \neq m)$ and the density of each network. The equation in (3) indicates that the successful transmission probability decreases with the target SIR β_m and the reference distance R_m.

To form a baseline for our evaluation of the performance of spectrum sharing, we define exclusive access as the scheme in which only network m uses the spectrum without the appearance of other networks. If network m is granted exclusive access, the expression in (4) is reduced to[2]

$$\widetilde{p}_m = \exp(-b_m \lambda_m), \quad \text{for } m = 0, 1, \ldots, M. \tag{7}$$

where we use the tilde to denote the case of exclusive access.

C. Throughput of Spectrum Sharing

The power allocation problem of interest is to maximize the throughput of spectrum sharing across all networks under QoS constraints of each network. We utilize the objective function that sums up the throughput of each network,

$$U = \sum_{m=0}^{M} U_m, \tag{8}$$

where U_m is the spatial throughput of network m in bits/s/Hz/m^{2}. Spatial throughput is defined as the product of the total rate per unit area and the corresponding probability that idealized transmission at that rate is successful (e.g., [24]);[3] i.e.,

$$U_m = \lambda_m \log_2(1 + \beta_m) p_m, \tag{9}$$

where $\log_2(1 + \beta_m)$ is the maximum achievable rate at a target SIR of β_m, and p_m is the successful transmission probability defined in (4) for the given β_m.

For a set of networks, the transmission power P_m of network m influences overall throughput via the successful transmission probability, p_m; cf. (8) and (9). An increase in the transmission power simultaneously strengthens the desired signal at the receiver and the interference to other networks, thereby resulting in a tradeoff. This study mainly aims to develop an efficient power allocation strategy that enables this tradeoff to be explored. To assess the performance of the proposed power allocation strategy, the baseline that we use is the throughput obtained when the PN is granted exclusive access to the available spectrum; i.e.,

$$\widetilde{U}_0 = \lambda_0 \log_2(1 + \beta_0) \widetilde{p}_0. \tag{10}$$

This change avoids repetition in the next section.

---

[2]Since we are considering an interference-limited scenario and since the successful transmission probability is defined in terms of an SIR target, the effect of power P_m on signal strength is offset by that on internal interference in the case of exclusive access. Therefore, probability $\widetilde{p}_m$ is independent of transmission power P_m. If the effect of noise is considered, then probability $\widetilde{p}_m$ depends on power P_m (e.g., [37]).

[3]This definition can be applied to calculate transmission capacity [38], $\lambda_m^{(\varepsilon)} \log_2(1 + \beta_m)(1 - \varepsilon)$, which defines the spectral efficiency per-unit-area for the maximum permissible network density that is subject to an outage constraint; i.e., $\lambda_m^{(\varepsilon)} = \sup\{\lambda_m : \mathbb{P}(\text{SIR} \leq \beta_m) \leq \varepsilon\}$. Unlike [38], the powers are the design variables and the network densities are given.

III. POWER ALLOCATION PROBLEM

In this section, we formulate the power allocation problem. We seek to allocate the power to the SNs so as to maximize the overall throughput gain that is subject to constraints on QoS by each network. For a given PN, we demonstrate that the joint power allocation problem for the SNs can be transformed into a convex optimization problem.

A. Formulation of the Power Allocation Problem

In the initial formulation of the problem, we determine the transmission power $P_1, P_2, \ldots, P_M$ of the SNs that maximize the increase in throughput over the case of exclusive access for the PN, $U - \widetilde{U}_0$, subject to the degradation of the successful transmission probability of each network over the probability when it has exclusive access, $\widetilde{p}_m - p_m$, being less than a prespecified constant δ_m. Given the transmission power of the PN, P_0, if we let $\mathbf{p} = [P_1, P_2 \ldots, P_M]^T$ denote the M-dimensional nonnegative power vector of the SNs, and $P_{\max,m}$ denote the maximum power constraint for the nodes in network m, the problem of interest can be formulated as follows:

$$\max_{\mathbf{p}} \ U - \widetilde{U}_0 \tag{11a}$$

$$\text{s.t. } \widetilde{p}_0 - p_0 \leq \delta_0, \tag{11b}$$

$$\widetilde{p}_m - p_m \leq \delta_m, \quad \text{for } m = 1, 2, \ldots, M, \tag{11c}$$

$$0 \leq P_m \leq P_{\max,m}, \quad \text{for } m = 1, 2, \ldots, M. \tag{11d}$$

where p_m is defined in (4), $\widetilde{p}_m$ in (7), U in (8) and $\widetilde{U}_0$ in (10). We point out that (11b) and (11c) can be viewed as soft interference constraints for underlay spectrum sharing [4], [5]. Since we focus on the effect of spectrum sharing, we constrain the differences in the values of the successful transmission probability, $\widetilde{p}_m - p_m$, rather than those in the values of probability itself, p_m. In that way, other networks will not be implicated if internal interference is the dominant cause of aggregate interference in network m. Furthermore, in addition to constraining the impact of interference on the PN using (11b), we also constrain the impact of interference on each SN using (11c). Although the transmission power of the PN, P_0, is given, the allocation of power to the SNs impact the successful transmission probability of the PN, p_0; cf. (4). Given the throughput of the PN, $\widetilde{U}_0$, the joint power allocation problem in (11) can be expressed explicitly as the following maximization problem of overall spectrum sharing throughput:

$$U^\star = \max_{\mathbf{p}} \ \sum_{m=0}^{M} a_m \exp\left[-b_m \sum_{n=0}^{M} \lambda_n \left(\frac{P_n}{P_m}\right)^{2/\alpha}\right] \tag{12a}$$

$$\text{s.t. } \sum_{n=0}^{M} \lambda_n \left(\frac{P_n}{P_m}\right)^{2/\alpha} \leq \eta_m, \text{ for } m=0,\ldots,M, \tag{12b}$$

$$0 \leq P_m \leq P_{\max,m}, \text{ for } m=1,2,\ldots,M, \tag{12c}$$

where

$$a_m = \lambda_m \log_2(1 + \beta_m) > 0, \tag{13}$$

$$\eta_m = -\frac{\ln\left[\exp(-b_m \lambda_m) - \delta_m\right]}{b_m}. \tag{14}$$

For future reference, we point out that $\eta_m > \lambda_m$ because

$$\frac{\lambda_m}{\eta_m} = -\frac{b_m \lambda_m}{\ln\left[\exp(-b_m \lambda_m) - \delta_m\right]} < -\frac{b_m \lambda_m}{\ln\left[\exp(-b_m \lambda_m)\right]} = 1. \tag{15}$$

B. Feasibility Condition

As the power allocation problem in (12) is a constrained optimization problem, it is of interest to determine whether there is a feasible power allocation, prior to attempting to solve the problem. As shown in the following proposition, necessary and sufficient conditions for the feasibility depend on the parameters of each network, such as network density, target SIR and maximum power.

Proposition 1: Problem (12) is feasible if and only if

$$\sum_{n=0}^{M} \frac{\lambda_n}{\eta_n} \leq 1 \text{ and } P_{\max,m} \geq \left[\frac{\lambda_0}{\left(1 - \sum_{n=1}^{M} \frac{\lambda_n}{\eta_n}\right)\eta_m}\right]^{\alpha/2} P_0.$$

Proof: See Appendix A. ∎

The feasibility condition in Proposition 1 guides the selection of network density λ_m, SIR threshold β_m, the limit on the decrement of successful transmission probability δ_m, and transmission distance R_m of network m, given the nature of the PN. In an individual network, we typically derive $\lambda_m/\eta_m < 1$ from (15). Proposition 1 demonstrates the necessary relation among these network properties that facilitates the coexistence of multiple networks.

Given the feasibility condition, the feasible region of the power allocated to each SN can be determined from the performance degradation constraints, as shown in the following proposition.

Proposition 2: The feasible region of secondary power in Problem (12) is $\left[\frac{\lambda_0}{(1-\sum_{n=1}^{M} \frac{\lambda_n}{\eta_n})\eta_m}\right]^{\alpha/2} P_0 \leq P_m \leq$ $\min\left\{P_{\max,m}, \left(\frac{\eta_0 - \lambda_0}{\lambda_m}\right)^{\alpha/2} P_0\right\}$, for $m = 1, 2, \ldots, M$.

Proof: See Appendix B. ∎

Since the target SIR threshold of the PN is positive, Propositions 1 and 2 guarantee the existence of the optimal solution to the power allocation problem of interest. This existence is based on the Weierstrass theorem [39] given that the feasible region of (12) is closed and bounded (as stated in Proposition 2), and the objective function in (12a) is continuous and differentiable.

Although (12) is a valid formulation of the problem of interest, it is not convex. Hence, the development of effective algorithms for solving it is hampered by the potential for multiple local optima. We indicate in the subsequent section that when the feasibility condition is satisfied, (12) can be transformed into a convex optimization problem wherein the variables are nearly decoupled. We then use this structure to develop an efficient solution algorithm in Section IV.

C. Transformation Into a Convex Optimization Problem

For $m = 0, 1, \ldots, M$, let r_m be the following scaled power allocation ratio for network m,

$$r_m = \frac{P_m^{2/\alpha}}{b_m \sum_{n=0}^{M} \lambda_n P_n^{2/\alpha}}, \tag{16}$$

where b_m is the positive parameter defined in (3). By substituting (16) into (12), we can formulate an equivalent optimization problem (17) with respect to the $(M+1)$-dimensional non-negative parameter vector $\mathbf{r} = [r_0, r_1, \ldots, r_M]^T$ that includes the scaled power allocation ratio of the PN.

$$\max_{\mathbf{r}} \sum_{m=0}^{M} a_m \exp\left(-\frac{1}{r_m}\right) \tag{17a}$$

$$\text{s.t.} \ \frac{1}{\eta_m b_m} - r_m \leq 0, \ \text{for } m = 0, 1, \ldots, M \tag{17b}$$

$$r_m - r_0 \frac{b_0}{b_m} \left(\frac{P_{\max,m}}{P_0}\right)^{2/\alpha} \leq 0, \ \text{for } m = 1, 2, \ldots, M \tag{17c}$$

$$\sum_{m=0}^{M} \lambda_m b_m r_m - 1 = 0. \tag{17d}$$

The expression in (17d) is obtained by forming the products $\lambda_m b_m$ and summing up both sides of (16) over the $M+1$ networks. As formalized in the following proposition, Problem (17) is a strictly convex optimization problem in $\mathbf{r}$ given that the successful transmission probability of each SN should not be unreasonably small.

Proposition 3: Under the feasibility condition in Proposition 1, Problem (17) is strictly convex if

$$\widetilde{p}_m > \exp(-2) + \delta_m, \quad \text{for } m = 0, 1 \ldots, M. \tag{18}$$

Proof: See Appendix C. ■

In most practical applications, the sufficient condition in Proposition 3 is unlikely to be restrictive. Condition (18) requires $\widetilde{p}_m - \delta_m > \exp(-2) \approx 0.1353, \forall m = 0, 1 \ldots, M$, where $\widetilde{p}_m - \delta_m$ is the lower bound limit on p_m as imposed by the constraints in (11b) and (11c). In most practical scenarios, an SN should not operate with a probability of success below 14% (i.e., at a probability of outage above 86%). Thus, the sufficient condition is unlikely to restrict the applicability of the convex formulation in (17). The strict convexity in Proposition 3 guarantees the uniqueness of the global optimum for the power allocation problem of interest.

The key to the convexity of (17) is the definition of r_m in (16). The M variables, $\{P_m\}_{m=1}^{M}$, that are coupled in (12a) and (12b) are replaced by $M+1$ almost decoupled variables, $\{r_m\}_{m=0}^{M}$ in (17a) and (17b). In the physical sense, the initial problem in (12) optimizes the power of each SN given that of the PN, whereas the transformed problem in (17) optimizes the power allocation ratio for each network (including the PN), which is the quantity that captures the performance of each network individually.

One approach to solving (17) is to employ general-purpose tools for convex optimization, such as interior-point methods [40]. Given the primary power P_0, the globally optimal secondary power P_m can then be obtained from the optimal solution to (17), $\mathbf{r}^\star = [r_0^\star, r_1^\star, \ldots, r_M^\star]^T$, by employing (16). This approach is summarized in Algorithm 1.

Algorithm 1 Using general-purpose tools

1: Check feasibility condition in Proposition 1. If feasible, then proceed, otherwise report infeasibility.
2: Solve (17) using a general-purpose tool like an interior-point method, and obtain the globally optimal $\mathbf{r}^\star = [r_0^\star, r_1^\star, \ldots, r_M^\star]^T$ and the associated maximum spatial throughput of spectrum sharing $U^\star = \sum_{m=0}^{M} a_m \exp(-(r_m^\star)^{-1})$.
3: The optimal secondary transmission power can be obtained using:

$$P_m^\star = \left(\frac{r_m^\star b_m}{r_0^\star b_0}\right)^{\alpha/2} P_0, \quad \text{for } m = 1, 2, \ldots, M, \tag{19}$$

where b_m is defined in (3).

IV. QUASI-CLOSED-FORM POWER ALLOCATION STRATEGY

Algorithm 1 efficiently solves the problem of total throughput under QoS constraints in (12). However, employing a general-purpose solver to solve (17) is not necessarily the most efficient approach, especially given a large number of spectrum sharing networks, M. In this section, we consider the case in which $P_{\max,m}$ is large enough to avoid activating the upper bound in (12c), or, equivalently, that in (17c). As shown in Proposition 2, this situation occurs when

$$P_{\max,m} \geq \left(\frac{\eta_0 - \lambda_0}{\lambda_m}\right)^{\alpha/2} P_0, \quad \text{for } m = 1, 2, \ldots, M. \tag{20}$$

In this case, by substituting (17b) into (17d) it can be shown that (17) is feasible if and only if $\sum_{n=0}^{M} \frac{\lambda_n}{\eta_n} \leq 1$ (a simpler condition than that in Proposition 1). By carefully inspecting (17b), we observe that the variables are coupled only in the single constraint in (17d), and that some components of the optimal solution lie on the boundary of $r_m^\star = \frac{1}{\eta_m b_m}$, whereas the others satisfy $r_m^\star > \frac{1}{\eta_m b_m}$. This observation suggests that a specialized algorithm or even a quasi-closed-form solution may be obtained. In this light, we generate some formal results in relation to the structure of the optimal solution.

First, we analyze a special case in which the equality of (17b) holds for every $r_m^\star$.

Proposition 4: Under the condition in (20), the optimal power allocation ratio of network m is

$$r_m^\star = \frac{1}{\eta_m b_m}, \ \text{for } m = 0, 1, \ldots, M, \tag{21}$$

if and only if

$$\sum_{n=0}^{M} \frac{\lambda_n}{\eta_n} = 1. \tag{22}$$

Proof: See Appendix D. ■

Actually, the optimal solution shown in Proposition 4 is the unique solution to (17) given (22), for any set $\{P_{\max,m}\}_m$ for which the problem is feasible. This can be seen from Proposition 2, where the upper bound on P_m is equal to the lower bound when (23) holds.

Given the relationship between the optimal secondary transmission power for (12) and the optimal solution to (17), as shown in (19), we arrive at the following corollary that essentially establishes a closed-form strategy for secondary power allocation under the special condition in (22).

Corollary 1: Under the condition in (20), if $\sum_{n=0}^{M} \frac{\lambda_n}{\eta_n} = 1$, the optimal secondary transmission power is

$$P_m^\star = \left(\frac{\eta_0}{\eta_m}\right)^{\alpha/2} P_0, \; for \; m = 1, 2, \ldots, M. \tag{23}$$

To analyze the other feasible case, namely when $\sum_{n=0}^{M} \frac{\lambda_n}{\eta_n} < 1$, we take advantage of the decoupling of the variables in all but one constraint of (17), and show that we can eventually obtain a quasi-closed-form optimal solution.

Let us define

$$c_m = \frac{a_m b_m \eta_m^2}{\lambda_m} \exp(-\eta_m b_m), \tag{24}$$

$$d_m = \frac{b_m \lambda_m}{a_m}, \tag{25}$$

$$F(x) = \frac{1}{x^2} \exp\left(-\frac{1}{x}\right), \tag{26}$$

$$G_i(x) = \sum_{k=0}^{i} \lambda_{m_k} b_{m_k} F^{-1}(x d_{m_k}) + \sum_{k=i+1}^{M} \left(\frac{\lambda_{m_k}}{\eta_{m_k}}\right) - 1, \tag{27}$$

and re-index the networks using $\{m_k\}$ instead of $\{m\}$ such that

$$c_{m_k} \geq c_{m_{k+1}}, \; \text{for all } k = 0, 1, \ldots, M-1. \tag{28}$$

Then, we arrive at the following proposition.

Proposition 5: Under the condition in (20), if $\sum_{n=0}^{M} \frac{\lambda_n}{\eta_n} < 1$, a quasi-closed-form solution to (17) is

$$r_{m_k}^\star = \begin{cases} F^{-1}\left(\mu^{(i-1)} d_{m_k}\right), & \text{for } k = 0, \ldots, i-1 \\ \frac{1}{\eta_{m_k} b_{m_k}}, & \text{for } k = i, \ldots, M, \end{cases} \tag{29}$$

where $\mu^{(i)}$ is the root of $G_i(\mu) = 0$ that satisfies $\mu^{(i-1)} < c_{m_{i-1}}$ and $\mu^{(i)} \geq c_{m_i}$, $i \in \{1, \ldots, M+1\}$.

Proof: See Appendix E. ∎

Note that if $i = M+1$ in Proposition 5, then all of the optimal components satisfy $r_m^\star > \frac{1}{\eta_m b_m}$ for all $m = 0, 1, \ldots, M$.

As the relationship between $P_m^\star$ and $r_m^\star$ in (19) still holds, we can derive the optimal power strategy for the SNs in a quasi-closed-form by applying the analysis in this section. The resultant power allocation strategy is summarized in Algorithm 2. This algorithm is advantageous over Algorithm 1 in that only a single Lagrange multiplier, μ, should be determined in place of the $(M+1)$-dimensional vector $\mathbf{r}$ in Algorithm 1. Once the optimal μ has been obtained, the optimal values for r_{m_k} can be calculated using (29). Furthermore, after sorting the networks according to (28), Algorithm 2 requires no more than $M+1$ iterations to determine the critical number i, and at each
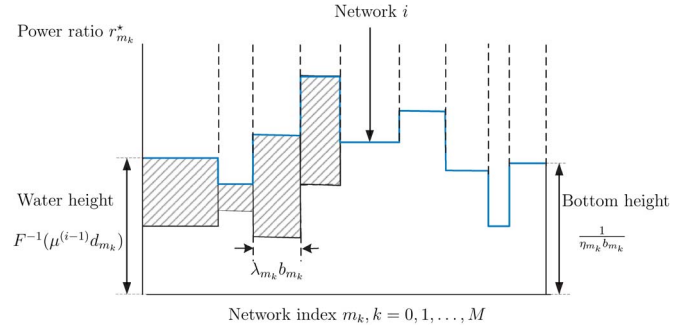

Fig. 2. Illustration of the process of obtaining solution to (17) can be interpreted as the water-filling process. The reservoirs are indexed by decreasing order of $\{c_{m_k}\}$; the height of the bottom each reservoir is $\frac{1}{\eta_{m_k} b_{m_k}}$, which is the boundary of (17b). The width of each reservoir is $\lambda_{m_k} b_{m_k}$; cf. (17d). Consequently, if a reservoir contains water, the optimal value, $r_{m_k}^\star$, is the height of the water above the baseline, whereas if it does not contain water, $r_{m_k}^\star$ is the height of the bottom above the baseline. Furthermore, the total area occupied by the water and the bottom is $\sum_{m_k=0}^{M} \lambda_{m_k} b_{m_k} r_{m_k}^\star = 1$, cf. (17d).

iteration all that needs to be done is to find the root of a one-dimensional function $G_i(\mu) = 0$.

Algorithm 2 Quasi-closed-form solution

1: Check feasibility condition in Proposition 1, if feasible, then proceed, otherwise report infeasibility.
2: Re-index the networks using $\{m_k\}$ rather than $\{m\}$ according to (28).
3: **if** $\sum_{n=0}^{M} \frac{\lambda_n}{\eta_n} = 1$ **then**
4:   Determine $P_m^\star$ using Corollary 1;
5: **else if** $\sum_{n=0}^{M} \frac{\lambda_n}{\eta_n} < 1$
6:   Determine $r_{m_k}^\star$ using Proposition 5;
7:   Determine $P_m^\star$ using (19);
8: **end if**.
9: The maximum spatial throughput is $U^\star = \sum_{m=0}^{M} a_m \exp\left(-\frac{1}{r_m^\star}\right)$.

Algorithm 2 also admits a water-filling interpretation. In particular, we can compare the process of optimizing $\mathbf{r}^\star$ with the process of pouring water into $M+1$ adjacent, indexed, self-contained reservoirs with uneven bottoms, as illustrated in Fig. 2:

a) For each of the $M+1$ reservoirs, set up a solid bottom up to height $\frac{1}{\eta_{m_k} b_{m_k}}$ and width $\lambda_{m_k} b_{m_k}$.
b) By computing $\mu^{(i)}$ and comparing $\mu^{(i)}$ with c_{m_i} based on Proposition 5, we can determine the critical threshold i, which is the largest number of self-contained reservoirs that actually contain water.
c) Pour water into each of the self-contained reservoirs, from reservoir 0 up to reservoir $i-1$, until water height (including the bottom) rises to $F^{-1}(\mu^{(i-1)} d_{m_k})$, $k = 0, \ldots, i-1$.
d) The water height above the baseline on the reservoir $\{m_k\}$, $k = 0, \ldots, i-1$, which contains water, and the bottom height above the baseline on the reservoir $\{m_k\}$,

TABLE I
SPECTRUM SHARING AMONG MULTIPLE POISSON NETWORKS

Number of networks $M+1$	Optimal power $\mathbf{p}^\star = [P_1^\star, \ldots, P_M^\star]$	Scaled power summation $t = \sum_{n=0}^{M} \lambda_n (P_n^\star)^{2/\alpha}$	Throughput of each network $[U_0^\star, U_1^\star, \ldots, U_M^\star]$	Improvement in the throughput of spectrum sharing $(U^\star - \widetilde{U}_0)/\widetilde{U}_0 \times 100\%$	Reduction in the throughput of the PN $(\widetilde{U}_0 - U_0^\star)/\widetilde{U}_0 \times 100\%$
2	4.3	8.4×10^{-5}	$[6.6, 2.2] \times 10^{-5}$	32.2%	1.0%
3	$[4.3, 5.3]$	1.3×10^{-4}	$[6.5, 2.2, 4.9] \times 10^{-5}$	101.7%	3.2%
4	$[2.4, 3.0, 3.6]$	1.7×10^{-4}	$[6.4, 2.1, 4.6, 7.6] \times 10^{-5}$	207.8%	5.2%
5 (max)	$[2.1, 1.0, 1.0, 1.2]$	1.7×10^{-4}	$[6.4, 2.1, 4.3, 6.9, 9.8] \times 10^{-5}$	337.1%	5.2%

$k = i, \ldots, M$, which does not contain water, gives optimal power ratio solution $r_{m_k}^\star$ to (17).

Note that the total amount of water is $1 - \sum_{m_k=0}^{M} \frac{\lambda_{m_k}}{\eta_{m_k}}$, cf. (17d). Therefore, if a new network joins in the spectrum sharing system, the amount of water that is available for distribution to the reservoirs is reduced. Indeed, Proposition 4 states the extreme situation in which no water is left (i.e., $\sum_{m_k=0}^{M} \frac{\lambda_{m_k}}{\eta_{m_k}} = 1$). The number of spectrum sharing networks then reaches a saturation point such that the addition of a network will generate intolerable interference (i.e., $\sum_{m_k=0}^{M} \frac{\lambda_{m_k}}{\eta_{m_k}} > 1$), and render the spectrum sharing problem infeasible (cf. Proposition 1).

To develop some insight into the extent to which the solution to the problem uses the available transmission power, we make the following definitions. Let t be the scaled power summation:

$$t = \sum_{n=0}^{M} \lambda_n P_n^{2/\alpha} \qquad (30)$$

$$t_{\max} = \eta_0 P_0^{2/\alpha} \qquad (31)$$

Suppose the sorted network index of the PN is m_τ according to (28), we have the following proposition for r_0, the scaled power ratio of the PN, defined in (16).

Proposition 6: Under the condition in (20), if $\sum_{n=0}^{M} \frac{\lambda_n}{\eta_n} < 1$, the primary power ratio satisfies

$$\frac{1}{\eta_0 b_0} \le r_0 \le \frac{1 - \sum_{n=1}^{M} \frac{\lambda_n}{\eta_n}}{\lambda_0 b_0}. \qquad (32)$$

If $\mu^{(\tau)} \ge c_{m_\tau}$, then the optimal primary power ratio is $r_0^\star = \frac{1}{\eta_0 b_0}$, and the maximized scaled power summation is reached, i.e., $t = t_{\max}$, where t and $t_{\max}$ are defined in (30) and (31), respectively.

Proof: See Appendix F. ∎

With the aid of Fig. 2, we can gain insight from Proposition 6 in the following way. Suppose only a few networks share the spectrum, such that the water level for the reservoir denoting each network is non-zero. New networks then join the spectrum sharing system one by one. As each network joins the system, the sorted network index changes; cf. (28). Once the index of the PN becomes the critical threshold, i.e., $\tau = i$, the scaled power summation t is maximized according to Proposition 6, i.e., $t = t_{\max}$. The generated number of networks is therefore the minimal number of networks that utilize all of the available power is utilized. Moving forward, any additional networks maintain $\tau \ge i$. This phenomenon is demonstrated by the numerical results in Table I of Section V.

In the current section, we present a quasi-closed-form solution for the case that $P_{\max,m} \ge (\frac{\eta_0 - \lambda_0}{\lambda_m})^{\alpha/2} P_0$. In practice, we can first solve the power allocation problem without any power constraints using Algorithm 2. If the optimal solution meets the actual power constraints of devices, this solution can be used directly. If it violates these constraints, we can then incorporate the power constraints into the formulation and take advantage of Algorithm 1.

V. NUMERICAL RESULTS AND DISCUSSION

In this section, we evaluate the performance of the proposed power allocation strategy and examine the effects of system parameters on spectrum sharing through some numerical experiments.

A. Multiple Spectrum Sharing Networks

In this subsection, we investigate scenarios that involve one PN and a maximum of four SNs ($M = 1, 2, 3, 4$). The following parameters are used [24]: network densities are $\lambda_0 = 2 \times 10^{-5} \mathrm{m}^{-2}$ and $\lambda_m = m \times 10^{-5} \mathrm{m}^{-2}$, for $m = 1, 2 \ldots, M$; the path-loss exponent is $\alpha = 4$; the reference transmission distances are $R_m = 10$ m, for $m = 0, 1 \ldots, M$; the transmission power of the PN is $P_0 = 10$; the target SIR thresholds are $\beta_0 = 10$, $\beta_m = 3 + m$, for $m = 1, 2 \ldots, M$; and the decrement bounds of the successful transmission probabilities are $\delta_m = 5\% \times (m+1)$, for $m = 0, 1, \ldots, M$. Given these parameters, the successful transmission probability of the PN with exclusive access, defined in (7), is $\widetilde{p}_0 \approx 0.97$. At present, we do not include the power constraints. The effects of additional power constraints will be discussed later in Section V-B.

As shown in Table I, spectrum sharing using the proposed power allocation strategy significantly enhances the maximum spectrum sharing throughput $U^\star$, which is defined in (12). (Recall that Algorithms 1 and 2 generate the same optimal power allocation $\mathbf{p}^\star$.) This has been achieved while explicitly specifying that the degradation in the throughput of each individual network due to spectrum sharing is comparatively small; cf. (11). Table I demonstrates that the throughput gain grows with the number of networks. This result is consistent with the intuition that spectrum utilization efficiency is enhanced when numerous networks coexist. As per the finding of Proposition 1, we observe that the maximum number of spectrum sharing networks is $M + 1 = 5$; i.e., $\sum_{n=0}^{4} \frac{\lambda_n}{\eta_n} \le 1 < \sum_{n=0}^{5} \frac{\lambda_n}{\eta_n}$, under the given parameter setting. Moreover, the scaled power summations are the same across four and five networks, as are the throughput decrements of the PN. This finding is ascribed to

TABLE II
COMPARISON BETWEEN (i) THE PROPOSED POWER ALLOCATION STRATEGY, (ii) DOUBLE POWER ALLOCATION AND
(iii) MAXIMUM POWER ALLOCATION ($P_{\max} = 10$) FOR SPECTRUM SHARING IN $M + 1 = 5$ NETWORKS

Power allocation $[P_1, \ldots, P_M]$	Scaled power summation t	Throughput of each network $[U_0, U_1, \ldots, U_M]$	Check QoS constraint of each network $[\widetilde{p}_0 - p_0 \leq \delta_0, \ldots, \widetilde{p}_M - p_m \leq \delta_M]$
(i) Proposed $[2.1, 1.0, 1.0, 1.2]$	1.7×10^{-4}	$[6.4, 2.1, 4.3, 6.9, 9.8] \times 10^{-5}$	$[\checkmark, \checkmark, \checkmark, \checkmark, \checkmark]$
(ii) Double $[4.2, 2.0, 2.0, 2.4]$	2.3×10^{-4}	$[6.2, 2.1, 4.4, 7.0, 10.0] \times 10^{-5}$	$[\times, \checkmark, \checkmark, \checkmark, \checkmark]$
(iii) Max $[10, 10, 10, 10]$	3.8×10^{-4}	$[5.7, 2.1, 4.5, 7.3, 10.3] \times 10^{-5}$	$[\times, \times, \checkmark, \checkmark, \checkmark]$

the fact that the scaled power summation is maximized, i.e., $t = t_{\max}$, and $r_0^\star = \frac{1}{\eta_0 b_0}$, as described following the presentation of Proposition 6.

Table II compares the performance of spectrum sharing using (i) the proposed power allocation strategy $[P_1^\star, \ldots, P_M^\star]$ with (ii) the case that all the networks are transmitting with double the proposed powers $[P_1, \ldots, P_M] = 2 \times [P_1^\star, \ldots, P_M^\star]$, and (iii) the case that all the networks are transmitting with their maximum power $P_1 = \ldots = P_M = P_{\max} = 10$. The increases in the power of each network result in additional energy consumption per unit area, as reflected in t. However, the additional power consumption does not improve overall spectrum sharing. A comparison of the throughput of each network $[U_0, U_1, \ldots, U_M]$ under each power allocation strategy indicates that larger powers increase the throughput of some individual networks but decrease that of others. This finding is expected, and is ascribed to the fact that larger power strengthens the desired signal, but also generates greater interference. In particular, using larger powers invalidates the QoS constraints (11b) and (11c) on the successful transmission probability of some of the networks, including the PN.

B. Effects of System Parameters

In this subsection, we examine the effects of network densities, target SIR thresholds, and transmission distances on spatial throughput. To give explicit insight, we consider spectrum sharing between two networks. When they are not specified in figures, the following parameters for these experiments are used [24]: the densities of the PN and the SN are $\lambda_0 = \lambda_1 = 5 \times 10^{-5} \mathrm{m}^{-2}$, the path-loss exponent is $\alpha = 4$, the reference transmission distance of each network is $R_0 = R_1 = 10$ m, the primary transmission power is $P_0 = 10$, the target SIR threshold of each network is $\beta_0 = \beta_1 = 5$, and the decrement bound of the successful transmission probability of each network is $\delta_0 = \delta_1 = 10\%$. These parameter settings satisfy $\sum_{n=0}^{1} \frac{\lambda_n}{\eta_n} < 1$ such that the power allocation problem is feasible (cf. Proposition 1), and Proposition 5 is applicable.

Fig. 3 depicts the increase in the maximum spatial throughput U with network densities λ_1 and λ_0. The spatial throughput U_0 of the PN decreases slightly with λ_1 and increases with λ_0. This result is attributed to the fact that high network density increases the spatial throughput of the associated network, as shown in (9). Meanwhile network density lowers the successful transmission probability of each network, as shown in (4). Note that the throughput U and U_0 reduce to $\widetilde{U}_0$ in the absence of SNs (i.e., $\lambda_1 = 0$), as exhibited in Fig. 3. This figure easily visualizes the improvement in throughput from spectrum sharing, and suggests that overall spectrum efficiency can be enhanced by allowing dense SNs to share the same spectrum while protect-
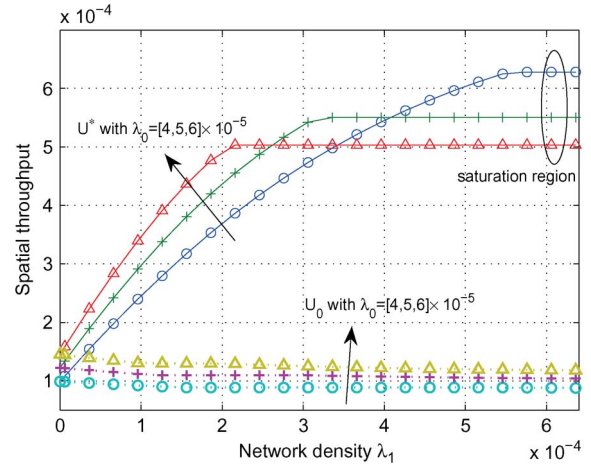

Fig. 3. Effect of the network densities λ_0 and λ_1 on the maximum spectrum sharing throughput of two networks (i.e., $U^\star$) and on the spatial throughput of the PN (i.e., U_0).

Fig. 4. Effect of SIR thresholds β_0 and β_1 on the maximum spectrum sharing throughput of two networks (i.e., $U^\s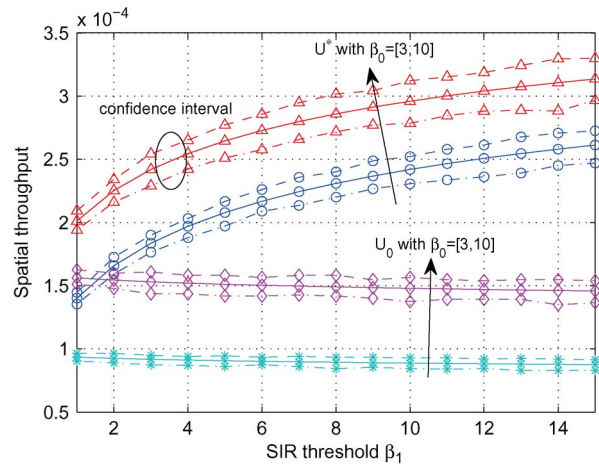tar$) and on the spatial throughput of the PN (i.e., U_0). To validate our experiments, the confidence intervals are plotted. These confidence intervals are typical of those in the other experiments.

ing the PN. Under the feasibility condition (cf. Proposition 1), throughput also increases with the density of the PN, λ_0. Small λ_0 allows large λ_1 and thus facilitates effective spectrum sharing through power optimization, until spectrum sharing reaches the saturation region at which the density of the SN becomes so high that the feasibility condition becomes active.

It can be seen from the Fig. 4 that the maximum throughput of spectrum sharing increases with large target SIR thresholds β_0 and β_1, and the spatial throughput U_0 of the PN increases with β_0 and decreases slightly with β_1. This finding is attributed to the fact that even though an increase in the target SIR threshold decreases the successful transmission probability
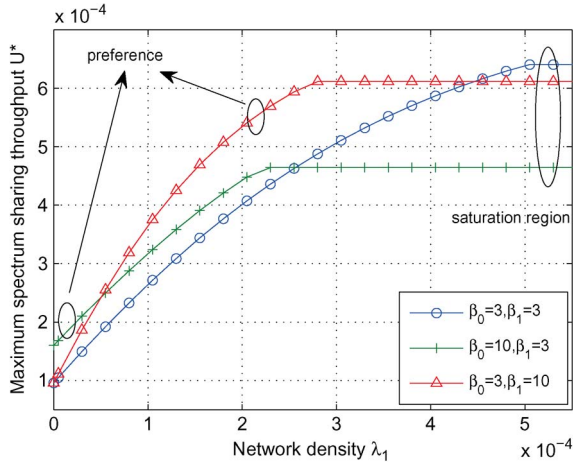
Fig. 5.   Effect of SIR thresholds β_0 and β_1 on the maximum throughput of the spectrum sharing between two networks with varying density λ_1 of SN, where $\lambda_0 = 5 \times 10^{-5} \text{m}^{-2}$.

Fig. 7.   Effects of the power constraints in (11d) and thermal noise on the maximum throughput of spectrum sharing between two networks (SNR = 20 dB), and a comparison with a power allocation strategy derived from [41].
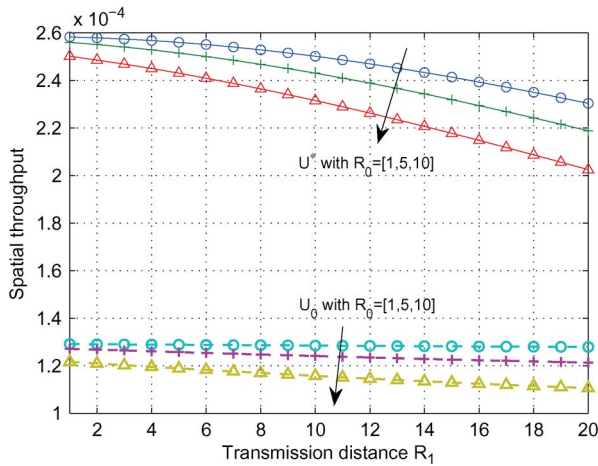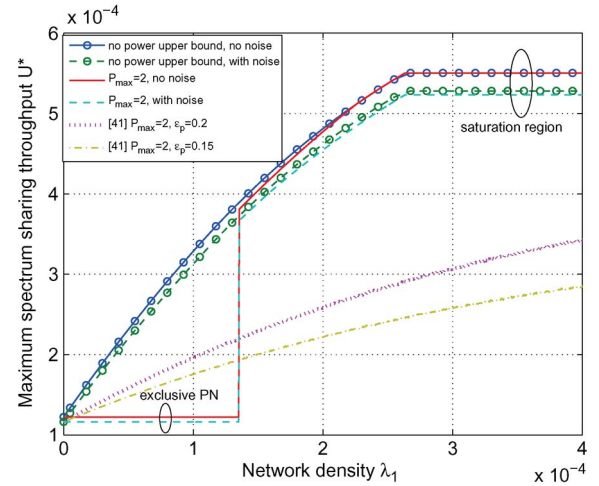

Fig. 6.   Effect of transmission distances R_0, R_1 on the maximum throughput of the spectrum sharing between two networks (i.e., $U^\star$) and on that of the PN (i.e., U_0).

defined in (4), the improvement in the data rate, $\log_2(1+\beta_m)$, predominantly affects the throughput. Notably, a large target SIR threshold for the PN, β_0, limits the aggregate interference from the SNs, thereby reducing spectrum sharing opportunities. By contrast, an increase in the target SIR threshold of the SN, β_1, consumes much secondary transmission power, thus generating additional interference to the PN. The influence of this interference is constrained (cf. (11b)); hence the setting of SIR thresholds involves a tradeoff. As shown in Fig. 5, we recommend increasing the SIR threshold of the PN when the network density of the SN is small compared to that of the PN in order for maximization of spectrum sharing throughput (i.e., the spatial throughput of the PN dominates the throughput of spectrum sharing), and we recommend increasing the SIR threshold of the SN when the network density of the SN is large. Fig. 5 also shows that small β_0 allows large λ_1 (cf. Proposition 1) and thus large $U^\star$ in the saturation region.

Fig. 6 plots the decrease of spatial throughput U and U_0 with the variation of transmission distances R_0 and R_1. An increase in the primary transmission distance R_0 decreases the strength of the primary received signal, which in turn limits the tolerance

of the PN for the interference from the SN. Consequently, for a given SIR threshold fewer spectrum sharing opportunities are available when the primary transmission distance R_0 is large. For a given SIR target, a large secondary transmission distance R_1 requires substantial secondary transmission power and thus generates additional interference towards the PN. Since the impact of this interference is constrained through the limit on the degradation in the successful transmission probability, the spectrum sharing opportunities are limited.

Fig. 7 shows the effects of the power constraints and thermal noise power on the spectrum sharing strategy, as the density of the SN, λ_1, changes. Since the feasible region of the secondary transmission power is (cf. Proposition 2) $[\lambda_0/(\eta_1 - \lambda_1)]^{\alpha/2}P_0 \leq P_1 \leq \min\{P_{\max}, [(\eta_0 - \lambda_0)/\lambda_1]^{\alpha/2}P_0\}$, where $P_{\max}$ denotes the power-constraint on the secondary nodes, spectrum sharing under the specified degradation constraints becomes infeasible whenever $P_{\max} < [\lambda_0/(\eta_1 - \lambda_1)]^{\alpha/2}P_0$ (cf. Proposition 1). In that case, the spectrum sharing system reduces to exclusive access for the PN. This can be seen for the cases of low-density SNs (i.e., low values of λ_1) in Fig. 7. Mathematically, this finding is attributed to the fact that η_1 is related to λ_1 by definition; cf. (14). Physically, $\tilde{p}_1$ is large when λ_1 is small; hence, p_1 requires a high power P_1 to limit the gap of $\tilde{p}_1 - p_1$. As a result, the constraint $P_1 \leq P_{\max}$ may induce infeasibility. Given intermediate values of λ_1, the spectrum sharing problem is feasible but the constraint imposed by $P_{\max}$ may still limit the throughput because the feasible set is smaller than that without power constraints (cf. Proposition 2). As λ_1 increases, the impact of $P_{\max}$ decreases, as observed in the noise free case in Fig. 7. Given large values of λ_1, $P_{\max} > [(\eta_0 - \lambda_0)/\lambda_1]^{\alpha/2}P_0$, the power constraint becomes inactive, and the optimal solution to the power constrained problem is the same as that of the problem without power constraints. Physically, power P_1 decreases to constrain the inference generated from a high λ_1. In Fig. 7, we also illustrate the impact of thermal noise on the throughput of the proposed power allocation strategy (which ignores thermal noise). In this case, the variance of thermal noise, σ^2, is set so that the expected signal-to-noise ratio (SNR)

at the reference node is 20 dB in the absence of interference. As is apparent from the figure, when the thermal noise is at this level the performance of the networks is dominated by the interference and hence the thermal noise has only a marginal impact on performance.

Fig. 7 also compares the performance of the proposed power allocation strategy for networks (in which multiple nodes are randomly deployed) with a strategy derived from a recent study for two transmitter-receiver pairs [41]. As demonstrated in this figure, the strategy derived from [41] provides higher throughput at the cost of large outage probabilities for small λ_1, and our proposed power allocation strategy provides higher throughput for large λ_1 because our design considers the aggregate interference from coexisting users. To describe the comparison in more detail, we observe that the work in [41] develops a power allocation strategy for an isolated interference channel with two transmitter-receiver pairs, one of which is designated the primary, the other is designated the secondary. The secondary transmitter is provided with full knowledge of its channel to the secondary receiver and of the channel from the PT to the secondary receiver. This is substantially more information than what is made available in the systems that we consider. Nevertheless, the objective of the power allocation strategy in [41], namely optimizing the achievable rate of the secondary link subject to the outage probability of the primary link being less than ε_p, is somewhat related to the problem we have considered. In addition to the differences in the CSI assumptions, a key difference is that [41] optimizes the achievable rate (in bits/sec/Hz) of the single secondary link, whereas we optimize the spatial throughput (in bits/sec/Hz/unit area) for Poisson networks. In the comparison in Fig. 7 we have applied the powers obtained for the primary and secondary links (using the channels and distances in [41]) to the PN and SNs (under our setting). For small λ_1 (when feasibility condition of proposed strategy is active), the strategy based on [41] provides higher throughput at the cost of larger outage probabilities. Indeed, only the outage probability of the single primary link is bounded in [41]. In particular, given the choice of $\varepsilon_p = 0.15$ in [41], the successful transmission probability of the PN, p_0, is constrained to be less than 0.85 when accounting for the interference from coexisting users in our scenario. In contrast, in the proposed strategy, we constrain the successful transmission probability degradation of both the PN ($\widetilde{p}_0 - p_0 \leq \delta_0$) and the secondary network ($\widetilde{p}_1 - p_1 \leq \delta_1$). In particular, given the parameters in our experiment, our strategy guarantees $p_0 \geq 0.85$. For large λ_1 (when the aggregate interference is large), the proposed power allocation strategy provides higher throughput because our strategy considers the coexistence of randomly deployed interferers whilst the strategy derived from [41] considers two transmitter-receiver pairs only.

In Fig. 8 we compare the performance of the proposed power allocation strategy for networks of given densities with that of the density optimization strategy for networks with a given power allocation proposed in [24]. As shown, by varying the design parameters (powers in our case, densities in the case of [24]) a range of different throughputs can be achieved. When the design parameters are set to their optimal values, the methods achieve a common optimal throughput (the stars
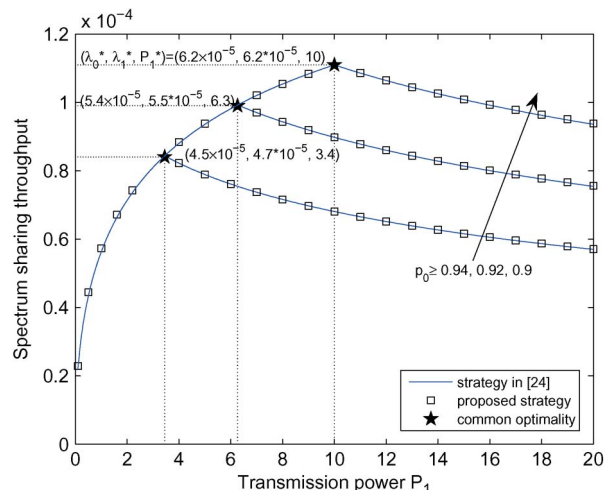

Fig. 8. Comparison of the power allocation strategy proposed in this work and the density optimization strategy proposed in [24] on the spectrum sharing throughput of two networks with different successful transmission probabilities ($\beta_0 = \beta_1 = 1, p_1 \geq 0.9$).

in Fig. 8). As an aside, we also observe from Fig. 8 that spectrum sharing throughput can be improved by reducing the successful transmission probability of the PN p_0. This is because additional interference is allowed when p_0 decreases.

VI. CONCLUSION

In this paper, we have developed a power allocation strategy for multiple spectrum sharing networks that depends on a model for the spatial distribution of nodes alone. This strategy allocates the transmission power in each secondary network to maximize the total throughput of the networks subject to probability-based QoS constraints in each network. By transforming the original power allocation problem into a convex formulation with respect to scaled power ratios, the problem can be solved efficiently. Moreover, we have derived a quasi-closed-form expression for the solution that has a water-filling interpretation. The numerical results have demonstrated that the proposed strategy significantly enhances throughput in various settings when the number of spectrum sharing networks increases up to the limit imposed by QoS feasibility. In addition, our interpretations have shown that appropriately setting the network densities and the target SIRs also increases overall spectrum sharing throughput with little degradation on the throughput of the PN.

The proposed power allocation strategy exploits features of the Poisson point process model that the nodes in the networks are assumed to follow. However, the fact that a large number of other point processes are based on the Poisson point process suggests that the principles of our approach could be extended to other models, such as the cluster models or the hard-core processes, which have guard zones; e.g., [18], [19]. The additional structure in those models may require increased coordination between the networks, but that the information required to facilitate that coordination would, once again, only need to be exchanged at the time scale of changes in the statistical model, as distinct from those in the instantaneous channel realizations.

APPENDIX

A. Proof of Proposition 1

Let $q_m = P_m^{2/\alpha}$ be the scaled transmission power of network m, and let $\mathbf{q} = [q_1, \ldots, q_M]^T$. This allows (12) to be written as

$$\max_{\mathbf{q}} \ \sum_{m=0}^{M} a_m \exp\left(-\frac{b_m}{q_m} \sum_{n=0}^{M} \lambda_n q_n\right) \qquad (33a)$$

$$\text{s.t.} \ \sum_{n=0}^{M} \lambda_n q_n \leq \eta_m q_m, \quad \text{for } m=0,1,\ldots,M \qquad (33b)$$

$$0 \leq q_m \leq P_{\max,m}^{2/\alpha}, \quad \text{for } m=1,2,\ldots,M \qquad (33c)$$

Necessity: Let $t = \sum_{n=0}^{M} \lambda_n q_n > \lambda_0 q_0 = t^{(0)}$. From (33b) and (33c), we find that $q_n \geq t^{(0)}/\eta_n = q_n^{(0)}$. Substituting $q_n^{(0)}$ into (33b), we have that $t \geq t^{(0)}[1 + \sum_{n=1}^{M}(\lambda_n/\eta_n)] = t^{(1)}$. After k iterations, $t \geq \lambda_0 q_0 + t^{(k-1)} \sum_{n=1}^{M}(\lambda_n/\eta_n) = t^{(0)}\{1 + \sum_{n=1}^{M}(\lambda_n/\eta_n) + \ldots + [\sum_{n=1}^{M}(\lambda_n/\eta_n)]^k\} = t^{(k)}$. Given that $t^{(k)}$ is bounded, we have $\sum_{n=1}^{M}(\lambda_n/\eta_n) < 1$ for all the SNs; hence, the lower bound on t converges to

$$t_{\min} = t^{(0)}\left[1 - \sum_{n=1}^{M}(\lambda_n/\eta_n)\right]^{-1}. \qquad (34)$$

By substituting $m = 0$ into (33b), we infer that $t \leq t_{\max} = \eta_0 q_0$. Since $t_{\min} \leq t_{\max}$, we further have $\sum_{n=0}^{M}(\lambda_n/\eta_n) \leq 1$, where this sum includes the PN. Consequently, a necessary condition for the feasibility of (12) is $\sum_{n=0}^{M}(\lambda_n/\eta_n) \leq 1$. Moreover, since $\frac{t_{\min}}{\eta_m} \leq \frac{t}{\eta_m} \leq q_m \leq P_{\max,m}^{2/\alpha}$, we have $P_{\max,m} \geq \left[\frac{\lambda_0}{(1-\sum_{n=1}^{M}\frac{\lambda_n}{\eta_n})\eta_m}\right]^{\alpha/2} P_0$.

Sufficiency: Given $\sum_{n=0}^{M}(\lambda_n/\eta_n) \leq 1$, we have $0 < t_{\min} = \lambda_0 q_0 \left[1 - \sum_{n=1}^{M}(\lambda_n/\eta_n)\right]^{-1} \leq t_{\max} = \eta_0 q_0$. Given $P_{\max,m} \geq (t_{\min}/\eta_m)^{\alpha/2} P_0$, we have $t_{\min} \leq P_{\max,m}^{2/\alpha}$. Then, there exists a feasible point $\mathbf{q} = [t/\eta_1, \ldots, t/\eta_m, \ldots, t/\eta_M]^T$ for $t_{\min} \leq t \leq \min\{P_{\max,m}^{2/\alpha}\eta_m, t_{\max}\}$. Thus, Problem (12) is feasible if $\sum_{n=0}^{M}(\lambda_n/\eta_n) \leq 1$ and $P_{\max,m} \geq (t_{\min}/\eta_m)^{\alpha/2} P_0$.

B. Proof of Proposition 2

From (33b), we have $\lambda_0 q_0 + \lambda_n q_n \leq t \leq t_{\max} = \eta_0 q_0$. Therefore, $q_m \leq \frac{\eta_0 - \lambda_0}{\lambda_m} q_0$. From (33b) and (33c), we have $\frac{t_{\min}}{\eta_m} \leq \frac{t}{\eta_m} \leq q_m \leq P_{\max,m}^{2/\alpha}$, where $t_{\min}$ is defined in (34). The bounds on P_m are then obtained using $q_m = P_m^{2/\alpha}$.

C. Proof of Proposition 3

Let $f(r_m) = \exp(-r_m^{-1})$. Then, $f''(r_m) = r_m^{-3}\exp(-r_m^{-1})(r_m^{-1} - 2)$. From (17b), $r_m^{-1} \leq \eta_m b_m = -\ln[\exp(-b_m\lambda_m) - \delta_m]$. If $\widetilde{p}_m = \exp(-b_m\lambda_m) > \exp(-2) + \delta_m$, then $r_m^{-1} < 2$; hence, $f''(r_m) < 0$. Therefore, $f(r_m)$ is strictly concave and so is the objective function in (17a). The proof follows by observing that the constraints are linear.

D. Proof of Proposition 4

The necessary condition is established by substituting $r_m^\star = (\eta_m b_m)^{-1}$ into (17d). The sufficiency is presented as follows. We suppose $\exists \hat{m} \in \{0, 1, \ldots, M\}$ such that $r_{\hat{m}} > (\eta_{\hat{m}} b_{\hat{m}})^{-1}$. Then $1 \geq \sum_{n \neq \hat{m}} \lambda_n/\eta_n + \lambda_{\hat{m}} b_{\hat{m}} r_{\hat{m}} > \sum_{n=0}^{M}(\lambda_n/\eta_n)$, which contradicts the assumption.

E. Proof of Proposition 5

We prove this proposition with the following lemma.

Lemma 1: If i components of $\mathbf{r}^\star$ satisfy $r_m^\star > \frac{1}{\eta_m b_m}$, and if $M - i$ components satisfy $r_m^\star = \frac{1}{\eta_m b_m}$, then

$$\begin{cases} r_{m_k}^\star > \frac{1}{\eta_{m_k} b_{m_k}}, & \text{for } k = 0, \ldots, i-1 \\ r_{m_k}^\star = \frac{1}{\eta_{m_k} b_{m_k}}, & \text{for } k = i, \ldots, M. \end{cases} \qquad (35)$$

Proof: First, we list the Karush-Kuhn-Tucker (KKT) optimality conditions of (17).

$$-\frac{a_m}{r_m^2}\exp\left(-\frac{1}{r_m}\right) - \nu_m + \mu\lambda_m b_m = 0, \text{ for } m = 0, 1, \ldots, M, \qquad (36a)$$

$$\frac{1}{\eta_m b_m} - r_m \leq 0, \text{ for } m = 0, 1, \ldots, M, \qquad (36b)$$

$$\sum_{m=0}^{M} \lambda_m b_m r_m - 1 = 0, \qquad (36c)$$

$$\nu_m \geq 0, \text{ for } m = 0, 1, \ldots, M, \qquad (36d)$$

$$\nu_m\left(\frac{1}{\eta_m b_m} - r_m\right) = 0, \text{ for } m = 0, 1, \ldots, M, \qquad (36e)$$

where $\nu_m, m = 0, 1, \ldots, M$ are the Lagrange multipliers for the inequalities in (17b), and μ is the Lagrange multiplier for the equality constraint (17d).

The proof proceeds by contradiction. Supposing that $r_{m_{\underline{k}}} = \frac{1}{\eta_{m_{\underline{k}}} b_{m_{\underline{k}}}}$, for $0 \leq \underline{k} \leq i-1$; and that $r_{m_{\overline{k}}} > \frac{1}{\eta_{m_{\overline{k}}} b_{m_{\overline{k}}}}$, for $i \leq \overline{k} \leq M$. Then, according to (36e), we have $\nu_{m_{\overline{k}}} = 0$. From (25), (26), and (36a), we have $F(r_{m_{\overline{k}}}) = \mu d_{m_{\overline{k}}}$. As $F(x) = f'(x)$, where $f(x)$ is defined in Appendix C, $F(r_m)$ is a monotonic decreasing function. Thus, an inverse function exists and is monotonic decreasing. Therefore,

$$r_{m_{\overline{k}}}^\star = F^{-1}\left(\mu d_{m_{\overline{k}}}\right), \qquad (37)$$

$$\mu = \frac{F\left(r_{m_{\overline{k}}}\right)}{d_{m_{\overline{k}}}} < \frac{F\left(\frac{1}{\eta_{m_{\overline{k}}} b_{m_{\overline{k}}}}\right)}{d_{m_{\overline{k}}}} = c_{m_{\overline{k}}}. \qquad (38)$$

Given (28), we know that $c_{m_{\overline{k}}} \leq c_{m_{\underline{k}}}$, and hence that $\mu < c_{m_{\underline{k}}}$. As a result,

$$r_{m_{\underline{k}}} = F^{-1}\left(\mu d_{m_{\underline{k}}}\right) > F^{-1}\left(c_{m_{\underline{k}}} d_{m_{\underline{k}}}\right) = \frac{1}{\eta_{m_{\underline{k}}} b_{m_{\underline{k}}}}. \qquad (39)$$

From the objective function in (17a), we can see that $r_{m_{\underline{k}}} > \frac{1}{\eta_{m_{\underline{k}}} b_{m_{\underline{k}}}}$ increases the value of (17a) over $r_{m_{\underline{k}}}^\star = \frac{1}{\eta_{m_{\underline{k}}} b_{m_{\underline{k}}}}$. Thus, a number of $i + 1$ optimal components satisfy $r_m^\star > \frac{1}{\eta_m b_m}$, thereby contradicting the assumption. ∎

Lemma 1 indicates that if we know the number of optimal components that are on the boundary, then we can determine which components are on the boundary simply by re-indexing the networks. Note that based on Proposition 4, at least one $\breve{m} \in \{0, 1, \ldots, M\}$ satisfies $r_{\breve{m}} > \frac{1}{\eta_{\breve{m}} b_{\breve{m}}}$ when $\sum_{n=0}^{M} \frac{\lambda_n}{\eta_n} < 1$. Considering $c_{m_0} \geq c_{m_1} \geq \ldots \geq c_{m_M}$ from (28), at least

$$r_{m_0}^{\star} > \frac{1}{\eta_{m_0} b_{m_0}}. \tag{40}$$

The remaining question is whether the critical number i of the optimal solution $\mathbf{r}^{\star}$ to (17) is the largest number of components that satisfy $r_m > \frac{1}{\eta_m b_m}$ among all the feasible $\mathbf{r}$.

The following lemma will help us determine the value of i. Let $U_{(j)}^{\star}$ denote the maximal value of objective function of (17) when $r_{m_k} = \frac{1}{\eta_{m_k} b_{m_k}}$, for $k = j+1, \ldots, M$, in addition to (17b) and (17d) holding for r_{m_k}, for $k = 0, \ldots, j$, i.e.,

$$U_{(j)}^{\star} = S_{(j)}^{\star} + \sum_{k=j+1}^{M} a_{m_k} \exp\left(-\eta_{m_k} b_{m_k}\right), \tag{41}$$

where

$$S_{(j)}^{\star} = \max \sum_{k=0}^{j} a_{m_k} \exp\left(-\frac{1}{r_{m_k}}\right)$$

$$\text{s.t. } r_{m_k} \geq \frac{1}{\eta_{m_k} b_{m_k}}, \quad \text{for } k = 0, \ldots, j,$$

$$\sum_{k=0}^{j} \lambda_{m_k} b_{m_k} r_{m_k} = 1 - \sum_{k=j+1}^{M} \frac{\lambda_{m_k}}{\eta_{m_k}}. \tag{42}$$

Lemma 2: $U_{(j+1)}^{\star} \geq U_{(j)}^{\star}$, for $j = 0, 1, \ldots, M-1$.

Proof: The relationship between $S_{(j+1)}^{\star}$ and $S_{(j)}^{\star}$ is $S_{(j+1)}^{\star} = S_{(j)}^{\star} + a_{m_{j+1}} \exp\left(-\eta_{m_{j+1}} b_{m_{j+1}}\right)$. We can prove that $U_{(j+1)}^{\star} \geq U_{(j)}^{\star}$ as follows: $U_{(j+1)}^{\star} - U_{(j)}^{\star} = S_{(j+1)}^{\star} + \sum_{k=j+2}^{M} a_{m_k} \exp(-\eta_{m_k} b_{m_k}) - S_{(j)}^{\star} - \sum_{k=j+1}^{M} a_{m_k} \exp(-\eta_{m_k} b_{m_k}) = S_{(j+1)}^{\star} - S_{(j)}^{\star} - a_{m_{j+1}} \exp(-\eta_{m_{j+1}} b_{m_{j+1}}) \geq 0$. ∎

Lemma 2 indicates that we should seek the largest value for i for which the KKT conditions admit a solution. If we re-index the networks, that value can be found from Lemma 1.

According to Proposition 4, at least (40) holds after re-indexing the networks when $\sum_{n=0}^{M} \frac{\lambda_n}{\eta_n} < 1$. Given (35) and (37), we have

$$r_{m_k}^{\star} = \begin{cases} F^{-1}\left(\mu d_{m_k}\right), & \text{for } k = 0, \ldots, i-1 \\ \frac{1}{\eta_{m_k} b_{m_k}}, & \text{for } k = i, \ldots, M; \end{cases} \tag{43}$$

then from (17d), we further have

$$G_{i-1}(\mu) = 0, \tag{44}$$

where μ is the Lagrange multiplier for (17d). The existence of the solution $\mu^{(i-1)}$ to (44) is a consequence of the feasibility of (17). The monotonicity of $F(r_m)$ leads to the monotonicity

of $G_i(\mu)$ and thus results in the uniqueness of $\mu^{(i-1)}$. Given the monotonic decreasing nature of $F(r_m)$, we can derive $\mu^{(i-1)} < c_{m_{i-1}}$ following the same procedure that resulted in (38).

Meanwhile, suppose $\mu^{(i)} < c_{m_i}$; we then have $r_{m_i} > \frac{1}{\eta_{m_i} b_{m_i}}$ because of (39). Then based on Lemma 1 and Lemma 2, a number of $i+1$ rather than i optimal components satisfy $r_m^{\star} > \frac{1}{\eta_m b_m}$, which contradicts the assumption of (35). Therefore, $\mu^{(i)} \geq c_{m_i}$.

F. Proof of Proposition 6

Based on the definition of r_m in (16) and of t in (30), and considering the relation $t_{\min} \leq t \leq t_{\max}$, where $t_{\max}$ and $t_{\min}$ are respectively defined in (31) and (34), the lower bound on r_0 is $r_0 = \frac{P_0^{2/\alpha}}{b_0 t} \geq \frac{P_0^{2/\alpha}}{b_0 t_{\max}} = \frac{1}{\eta_0 b_0}$, and the upper bound on r_0 is $r_0 = \frac{P_0^{2/\alpha}}{b_0 t} \leq \frac{P_0^{2/\alpha}}{b_0 t_{\min}} = \frac{1 - \sum_{n=1}^{M} \frac{\lambda_n}{\eta_n}}{\lambda_0 b_0}$. If $\mu^{(\tau)} \geq c_{m_\tau}$, $r_0^{\star}$ hits the boundary of (17b), as indicated in Proposition 5, i.e., $r_0^{\star} = \frac{1}{\eta_0 b_0}$. According to the definition of r_m, we have $t = t_{\max}$.

REFERENCES

[1] I. F. Akyildiz, W.-Y. Lee, M. C. Vuran, and S. Mohanty, "Next generation/dynamic spectrum access/cognitive radio wireless networks: A survey," *Comput. Netw.*, vol. 50, no. 13, pp. 2127–2159, Sep. 2006.

[2] Q. Zhao and B. M. Sadler, "A survey of dynamic spectrum access," *IEEE Signal Process. Mag.*, vol. 24, no. 3, pp. 79–89, May 2007.

[3] T. C. Clancy, "Formalizing the interference temperature model," *Wireless Commun. Mobile Comput.*, vol. 7, no. 9, pp. 1077–1086, Nov. 2007.

[4] A. Goldsmith, S. A. Jafar, I. Maric, and S. Srinivasa, "Breaking spectrum gridlock with cognitive radios: An information theoretic perspective," *Proc. IEEE*, vol. 97, no. 5, pp. 894–914, May 2009.

[5] R. Zhang, "On peak versus average interference power constraints for protecting primary users in cognitive radio networks," *IEEE Trans. Wireless Commun.*, vol. 8, no. 4, pp. 2112–2120, Apr. 2009.

[6] A. Ghasemi and E. S. Sousa, "Fundamental limits of spectrum-sharing in fading environments," *IEEE Trans. Wireless Commun.*, vol. 6, no. 2, pp. 649–658, Feb. 2007.

[7] L. B. Le and E. Hossain, "Resource allocation for spectrum underlay in cognitive radio networks," *IEEE Trans. Wireless Commun.*, vol. 7, no. 12, pp. 5306–5315, Dec. 2008.

[8] X. Kang, Y.-C. Liang, A. Nallanathan, H. K. Garg, and R. Zhang, "Optimal power allocation for fading channels in cognitive radio networks: Ergodic capacity and outage capacity," *IEEE Trans. Wireless Commun.*, vol. 8, no. 2, pp. 940–950, Feb. 2009.

[9] L. Musavian and S. Aissa, "Capacity and power allocation for spectrum-sharing communications in fading channels," *IEEE Trans. Wireless Commun.*, vol. 8, no. 1, pp. 148–156, Jan. 2009.

[10] I. Mitliagkas, N. D. Sidiropoulos, and A. Swami, "Joint power and admission control for ad-hoc and cognitive underlay networks: Convex approximation and distributed implementation," *IEEE Trans. Wireless Commun.*, vol. 10, no. 12, pp. 4110–4121, Dec. 2011.

[11] H. A. Suraweera, P. J. Smith, and M. Shafi, "Capacity limits and performance analysis of cognitive radio with imperfect channel knowledge," *IEEE Trans. Veh. Technol.*, vol. 59, no. 4, pp. 1811–1822, May 2010.

[12] H. Kim, H. Wang, S. Lim, and D. Hong, "On the impact of outdated channel information on the capacity of secondary user in spectrum sharing environments," *IEEE Trans. Wireless Commun.*, vol. 11, no. 1, pp. 284–295, Jan. 2012.

[13] A. G. Marques, X. Wang, and G. B. Giannakis, "Dynamic resource management for cognitive radios using limited-rate feedback," *IEEE Trans. Signal Process.*, vol. 57, no. 9, pp. 3651–3666, Sep. 2009.

[14] G. Zheng, K.-K. Wong, and B. Ottersten, "Robust cognitive beamforming with bounded channel uncertainties," *IEEE Trans. Signal Process.*, vol. 57, no. 12, pp. 4871–4881, Dec. 2009.

[15] E. Dall'Anese, S.-J. Kim, G. B. Giannakis, and S. Pupolin, "Power control for cognitive radio networks under channel uncertainty," *IEEE Trans. Wireless Commun.*, vol. 10, no. 10, pp. 3541–3551, Oct. 2011.

[16] P. Jia, M. Vu, T. Le-Ngoc, S.-C. Hong, and V. Tarokh, "Capacity- and Bayesian-based cognitive sensing with location side information," *IEEE J. Sel. Areas Commun.*, vol. 29, no. 2, pp. 276–289, Feb. 2011.

[17] B. Mark and A. Nasif, "Estimation of maximum interference-free power level for opportunistic spectrum access," *IEEE Trans. Wireless Commun.*, vol. 8, no. 5, pp. 2505–2513, May 2009.

[18] F. Baccelli and B. Blaszczyszyn, "Stochastic geometry and wireless networks: Volume I theory," *Found. Trends Netw.*, vol. 3, no. 3, pp. 249–449, 2009.

[19] F. Baccelli and B. Blaszczyszyn, "Stochastic geometry and wireless networks: Volume II applications," *Found. Trends Netw.*, vol. 4, no. 1, pp. 1–312, 2009.

[20] M. Haenggi, J. G. Andrews, F. Baccelli, O. Dousse, and M. Franceschetti, "Stochastic geometry and random graphs for the analysis and design of wireless networks," *IEEE J. Sel. Areas Commun.*, vol. 27, no. 7, pp. 1029–1046, Sep. 2009.

[21] H. ElSawy, E. Hossain, and M. Haenggi, "Stochastic geometry for modeling, analysis, design of multi-tier and cognitive cellular wireless networks: A survey," *IEEE Commun. Surveys Tuts.*, vol. 15, no. 3, pp. 996–1019, 2013.

[22] C. Yin, C. Chen, T. Liu, and S. Cui, "Generalized results of transmission capacities for overlaid wireless networks," in *Proc. IEEE ISIT*, Seoul, Korea, Jul. 2009, pp. 1774–1778.

[23] K. Huang, V. K. N. Lau, and Y. Chen, "Spectrum sharing between cellular and mobile Ad Hoc networks: Transmission-capacity trade-off," *IEEE J. Sel. Areas Commun.*, vol. 27, no. 7, pp. 1256–1267, Aug. 2009.

[24] J. Lee, J. G. Andrews, and D. Hong, "Spectrum-sharing transmission capacity," *IEEE Trans. Wireless Commun.*, vol. 10, no. 9, pp. 3053–3063, Sep. 2011.

[25] C.-H. Lee and M. Haenggi, "Interference and outage in Poisson cognitive networks," *IEEE Trans. Wireless Commun.*, vol. 11, no. 4, pp. 1392–1401, Apr. 2012.

[26] M. Xie, W. Zhang, and K.-K. Wong, "A geometric approach to improve spectrum efficiency for cognitive relay networks," *IEEE Trans. Wireless Commun.*, vol. 9, no. 1, pp. 268–281, Jan. 2010.

[27] A. Rabbachin, T. Q. S. Quek, H. Shin, and M. Z. Win, "Cognitive network interference," *IEEE J. Sel. Areas Commun.*, vol. 29, no. 2, pp. 480–493, Feb. 2011.

[28] W. Ren, Q. Zhao, and A. Swami, "Power control in cognitive radio networks: How to cross a multi-lane highway," *IEEE J. Sel. Areas Commun.*, vol. 27, no. 7, pp. 1283–1296, Sep. 2009.

[29] S. Lee, R. Zhang, and K. Huang, "Opportunistic wireless energy harvesting in cognitive radio networks," *IEEE Trans. Wireless Commun.*, vol. 12, no. 9, pp. 4788–4799, Sep. 2013.

[30] N. Golmie, N. Chevrollier, and O. Rebala, "Bluetooth and WLAN coexistence: Challenges and solutions," *IEEE Wireless Commun. Mag.*, vol. 10, no. 6, pp. 22–29, Dec. 2003.

[31] H. S. Dhillon, R. K. Ganti, F. Baccelli, and J. G. Andrews, "Modeling and analysis of K-tier downlink heterogeneous cellular networks," *IEEE J. Sel. Areas Commun.*, vol. 30, no. 3, pp. 550–560, Apr. 2012.

[32] H. ElSawy and E. Hossain, "On stochastic geometry modeling of cellular uplink transmission with truncated channel inversion power control," *IEEE Trans. Wireless Commun.*, vol. 13, no. 8, pp. 4454–4469, Aug. 2014.

[33] Z. Liu, T. Peng, Q. Lu, and W. Wang, "Transmission capacity of D2D communication under heterogeneous networks with dual bands," in *Proc. Int. Conf. CROWNCOM*, 2012, pp. 169–174.

[34] M. Song, C. Xin, Y. Zhao, and X. Cheng, "Dynamic spectrum access: From cognitive radio to network radio," *IEEE Wireless Commun. Mag.*, vol. 19, no. 1, pp. 23–29, Feb. 2012.

[35] X. Zhou and H. Zheng, "Trust: A general framework for truthful double spectrum auctions," in *Proc. IEEE INFOCOM*, Rio de Janerio, Brazil, Apr. 2009, pp. 999–1007.

[36] M. Haenggi and R. K. Ganti, "Interference in large wireless networks," *Found. Trends Netw.*, vol. 3, no. 2, pp. 127–248, 2008.

[37] R. Cai, W. Zhang, and P. C. Ching, "Spectrum sharing between random geometric networks," in *Proc. IEEE ICASSP*, Kyoto, Japan, Mar. 2012, pp. 3137–3140.

[38] S. Weber, J. G. Andrews, and N. Jindal, "An overview of the transmission capacity of wireless networks," *IEEE Trans. Commun.*, vol. 58, no. 12, pp. 3593–3604, Dec. 2010.

[39] W. Rudin and J. Cofman, *Principles of Mathematical Analysis*. New York, NY, USA: McGraw-Hill, 1964.

[40] S. Boyd and L. Vandenberge, *Convex Optimization*. Cambridge, U.K.: Cambridge Univ. Press, 2004.

[41] X. Gong, A. Ispas, G. Dartmann, and G. Ascheid, "Outage-constrained power allocation in spectrum sharing systems with partial CSI," *IEEE Trans. Commun.*, vol. 62, no. 2, pp. 452–466, Feb. 2014.

Ran Cai (S'11) received the B.Eng. degree (with the highest distinction) in electronic engineering from Beijing University of Posts and Telecommunications, Beijing, China, in 2010 and the Ph.D. degree in electronic engineering from The Chinese University of Hong Kong, Shatin, Hong Kong, in 2014.

She is currently with the Department of Electronic Engineering, Faculty of Engineering, The Chinese University of Hong Kong, as a Research Staff. From July 2011 to September 2011, she was a Visiting Ph.D. Student with the School of Electrical Engineering and Telecommunications, Faculty of Engineering, University of New South Wales, Sydney, Australia. From July 2012 to November 2012, she was a Visiting Ph.D. Student with the Department of Electrical and Computer Engineering, Faculty of Engineering, McMaster University, Hamilton, ON, Canada. Her research interests include signal processing and communications, particularly interference mitigation, resource allocation, and constrained optimization in wireless networks, as well as the application of stochastic geometry.

Jian-Kang Zhang (SM'09) received the B.S. degree in information science (mathematics) from Shaanxi Normal University, Xi'an, China, the M.S. degree in information and computational science (mathematics) from Northwest University, Xi'an, China, and the Ph.D. degree in electrical engineering from Xidian University, Xi'an, China.

He is currently an Associate Professor with the Department of Electrical and Computer Engineering, Faculty of Engineering, McMaster University, Hamilton, ON, Canada. He has held research positions with Harvard University, Cambridge, MA, USA, and with McMaster University. His research interests include the general area of signal processing, digital communication, signal detection and estimation, wavelet and time-frequency analysis, mainly emphasizing mathematics-based new technology innovation and exploration for a variety of signal processing and practical applications, and particularly, number theory, matrix theory, and linear algebra-based various kinds of signal processing. His current research focuses on transceiver designs for multiuser communication systems, coherent and non-coherent space–time signal and receiver designs for MIMO, and cooperative relay communications.

Dr. Zhang has served as an Associate Editor for the IEEE SIGNAL PROCESSING LETTERS. He is currently serving as an Associate Editor for the IEEE TRANSACTIONS ON SIGNAL PROCESSING and the *Journal of Electrical and Computer Engineering*. He was the corecipient of the IEEE Signal Processing Society's Best Young Author Award in 2008.

Timothy N. Davidson (M'96) received the B.Eng. (Hons. I) degree in electronic engineering from the University of Western Australia (UWA), Perth, Australia, in 1991 and the D.Phil. degree in engineering science from the University of Oxford, Oxford, U.K., in 1995.

He is a Professor with the Department of Electrical and Computer Engineering, Faculty of Engineering, McMaster University, Hamilton, ON, Canada, where he is currently serving as the Chair of the Department. Previously, he has served as the Acting Director of the School of Computational Engineering and Science, McMaster University for two years and as an Associate Director for three years. His research interests include the general areas of communications, signal processing, and control.

Dr. Davidson is a Registered Professional Engineer in the Province of Ontario. He has served as an Associate Editor of the IEEE TRANSACTIONS ON SIGNAL PROCESSING, the IEEE TRANSACTIONS ON WIRELESS COMMUNICATIONS, and the IEEE TRANSACTIONS ON CIRCUITS AND SYSTEMS II. He has also served as a Guest Coeditor of issues of the IEEE JOURNAL ON SELECTED AREAS IN COMMUNICATIONS and the IEEE JOURNAL OF SELECTED TOPICS IN SIGNAL PROCESSING. He was a General Cochair for the 2014 IEEE International Workshop on Signal Processing Advances in Wireless Communications and is a Technical Program Cochair for the 2014 IEEE Global Conference on Signal and Information Processing. He is also currently serving as the Chair of the IEEE Signal Processing Society's Technical Committee on Signal Processing for Communications and Networking. He was the recipient of the 1991 J. A. Wood Memorial Prize from UWA, the 1991 Rhodes Scholarship for Western Australia, and a 2011 Best Paper Award from the IEEE Signal Processing Society.

Wei Zhang (S'01–M'06–SM'11–F'15) received the Ph.D. degree in electronic engineering from The Chinese University of Hong Kong, Shatin, Hong Kong, in 2005.

In 2006–2007, he was a Research Fellow with the Department of Electronic and Computer Engineering, School of Engineering, The Hong Kong University of Science and Technology, Kowloon, Hong Kong. Since 2008, he has been with the School of Electrical Engineering and Telecommunications, Faculty of Engineering, University of New South Wales, Sydney, Australia, where he is an Associate Professor. His current research interests include cognitive radio, cooperative communications, space–time coding, and multiuser MIMO. He was the TPC Cochair of the Communications Theory Symposium of the IEEE International Conference on Communications, Kyoto, Japan, in 2011. He serves as the TPC Chair of the Signal Processing for Cognitive Radios and Networks Symposium in the 2nd IEEE Global Conference on Signal and Information Processing (GlobalSIP), Atlanta, GA, USA, in 2014. He is an Editor of the IEEE TRANSACTIONS ON WIRELESS COMMUNICATIONS and the IEEE JOURNAL ON SELECTED AREAS IN COMMUNICATIONS (Cognitive Radio Series). He was the recipient of the Best Paper Award at the 50th IEEE Global Communications Conference (GLOBECOM), Washington DC, USA, in 2007 and of the IEEE Communications Society Asia-Pacific Outstanding Young Researcher Award in 2009. He was elevated to IEEE Fellow in November 2014.

Kon Max Wong (LF'13) received the B.Sc.(Eng.), D.I.C., Ph.D., and D.Sc.(Eng.) degrees from the University of London, London, U.K., in 1969, 1972, 1974, and 1995, respectively, all in electrical engineering.

In 1969, he started working with Plessey Telecommunications Research Ltd., Ilford, U.K. In October 1970, he was on leave from Plessey, pursuing postgraduate studies and research with the Imperial College of Science and Technology, London, U.K. In 1972, he rejoined Plessey as a Research Engineer and worked on digital signal processing and signal transmission. In 1976, he joined the Department of Electrical Engineering, Technical University of Nova Scotia, Halifax, NS, Canada, and in 1981, he moved to the Department of Electrical and Computer Engineering, Faculty of Engineering, McMaster University, Hamilton, ON, Canada, where he has been a Professor since 1985; served as the Chairman of the Department in 1986–1987, 1988–1994, and 2003–2008; held the NSERC-Mitel Professor of Signal Processing in 2000–2003; and has been the Canada Research Chair in Signal Processing since 2004. In 1997–1999, he was on leave as a Visiting Professor with the Department of Electronic Engineering, Faculty of Engineering, The Chinese University of Hong Kong, Shatin, Hong Kong. He is the author or coauthor of over 250 papers in his areas of interest. His research interests include signal processing and communication theory.

Dr. Wong is a Fellow of the Institution of Electrical Engineers (IEE), the Royal Statistical Society, and the Institute of Physics. More recently, he has been also elected as a Fellow of the Canadian Academy of Engineering and the Royal Society of Canada. He was an Associate Editor of the IEEE TRANSACTIONS ON SIGNAL PROCESSING in 1996–1998 and served as the Chair of the Sensor Array and Multichannel Signal Processing Technical Committee of the IEEE Signal Processing Society in 2002–2004. He was the recipient of the IEE Overseas Premium for the Best Paper in 1989 and a corecipient of the IEEE Signal Processing Society's Best Young Author Awards in 2006 and 2008. He was the recipient of the Royal Academy of Engineering Distinguished Visiting Fellowship in 2009, the McMaster Engineering Faculty Lifetime Research Award in 2010, and the Alexander von Humboldt Research Award. He was a recipient of a medal presented by the International Biographical Centre, Cambridge, U.K., for his outstanding contributions to the research and education in signal processing in May 2000, and he was honored with the inclusion of his biography in the books *Outstanding People of the 20th Century* and *2000 Outstanding Intellectuals of the 20th Century*, published by IBC to celebrate the arrival of the new millennium.

P. C. Ching (F'11) received the B.Eng. (First Class Honors) and Ph.D. degrees from the University of Liverpool, Liverpool, U.K., in 1977 and 1981, respectively.

From 1981 to 1982, he was a Research Officer with the University of Bath, Bath, U.K. In 1982, he returned to Hong Kong and joined The Hong Kong Polytechnic University, Hung Hom, Hong Kong, as a Lecturer. Since 1984, he has been with the Department of Electronic Engineering, Faculty of Engineering, The Chinese University of Hong Kong (CUHK), Shatin, Hong Kong, where he is currently a Choh-Ming Li Professor of Electronic Engineering and was the Department Chair from 1995 to 1997, the Dean of Engineering from 1997 to 2003, and the Head of the Shaw College from 2004 to 2008. In 2004, he became the Director of the Shun Hing Institute of Advanced Engineering, CUHK. On August 1 2006, he assumed his new responsibility as the Pro-Vice Chancellor of CUHK. His research interests include adaptive digital signal processing, time-delay estimation and target localization, blind signal estimation and separation, automatic speech recognition, speaker identification/verification and speech synthesis, and advanced signal processing techniques for wireless communications. He is very active in promoting professional activities both in Hong Kong and overseas.

Dr. Ching is a Fellow of the Institution of Electrical Engineers (IEE), the HKIE, and the HKAES. He was a Council Member of the IEE, a past Chair of the IEEE Hong Kong Section, and an Associate Editor of the IEEE TRANSACTIONS ON SIGNAL PROCESSING from 1997 to 2000 and the IEEE SIGNAL PROCESSING LETTERS from 2001 to 2003. He was also a member of the Technical Committee of the IEEE Signal Processing Society from 1996 to 2004. He was appointed Editor-in-Chief of the *HKIE Transactions* between 2001 and 2004. He is also an Honorary Member of the editorial committee for the *Journal of Data Acquisition and Processing*. He has been instrumental in organizing many international conferences in Hong Kong, including the 1997 IEEE International Symposium on Circuits and Systems, where he was the Vice Chair, and the 2003 IEEE International Conference on Acoustics, Speech and Signal Processing, where he was the Technical Program Chair. He was the recipient of the IEEE Third Millennium Medal in 2000 and the HKIE Hall of Fame in 2010.